10-1-2011

A tight coupling between β_2Y97 and β_2F200 of the $GABA_A$ receptor mediates GABA binding

Phu N. Tran
Marquette University

Kurt T. Laha
Marquette University, kurt.laha@marquette.edu

David A. Wagner
Marquette University, david.wagner@marquette.edu

Accepted version. *Journal of Neurochemistry*, Vol. 119, No. 2 (October 2011): 283–293. DOI.

A Tight Coupling between β2y97 And β2f200 Of The $GABA_A$ Receptor Mediates GABA Binding

Phu N. Tran
Department of Biological Sciences, Marquette University, Milwaukee, WI
Kurt T. Laha
Department of Biological Sciences, Marquette University, Milwaukee, WI
David A. Wagner
Department of Biological Sciences, Marquette University, Milwaukee, WI

Abstract: The $GABA_A$ receptor is an oligopentameric chloride channel that is activated via conformation changes induced upon the binding of the endogenous ligand, GABA, to the extracellular inter-subunit interfaces. While dozens of amino acid residues at the α/β interface have been implicated in ligand binding, the structural elements that mediate ligand binding and receptor activation are not yet fully described. Here, double-mutant cycle analysis was employed to test for possible interactions between several arginines (α_1R67, α_1R120, α_1R132, and β_2R207) and two aromatic residues (β_2Y97 and β_2F200) that are present in the ligand-binding pocket and are known to influence GABA affinity. Our results show that neither α_1R67 nor

Journal of Neurochemistry, Vol. 119, No. 2 (October 2011): pg. 283-293. DOI.

α_1R120 is functionally coupled to either of the aromatics, while a moderate coupling exists between α_1R132 and both aromatic residues. Significant functional coupling between β_2R207 and both β_2Y97 and β_2F200 was found. Furthermore, we identified an even stronger coupling between the two aromatics, β_2Y97 and β_2F200, and for the first time provided direct evidence for the involvement of β_2Y97 and β_2F200 in GABA binding. As these residues are tightly linked, and mutation of either has similar, severe effects on GABA binding and receptor kinetics, we believe they form a single functional unit that may directly coordinate GABA.

Keywords: $GABA_A$ receptor, GABA binding, functional coupling

Introduction

The $GABA_A$ receptors are members of the ligand-gated ion channel (LGIC) superfamily, which also includes nicotinic acetylcholine, serotonin (5-HT_3), and glycine receptors. Each of the LGICs is activated by a unique endogenous ligand, binding of which leads to a specific activation pattern (i.e. opening and closing) of the intrinsic ion channel. It is the nature of these receptor-ligand interactions that defines the role each LGIC plays in information processing in the central nervous system. Consequently, it is of paramount importance to determine the molecular details of this process.

A profusion of studies have contributed to our understanding of the interaction between the $GABA_A$ receptors and their endogenous ligand, γ-aminobutyric acid (GABA). From these, it is clear that the GABA binding site is located at the interface of the α and β subunits (Cromer *et al.* 2002; Kash *et al.* 2004), and a multitude of amino acid residues that are both located at this interface and mediate GABA affinity have been identified (Lummis 2009). In addition, the general architecture of the binding site has been determined through homology modeling (Cromer *et al.* 2002). However, details of the molecular interactions that underlie the ligand-receptor interaction remain elusive.

A particularly intriguing possibility is that the positively charged amino group of GABA may interact with an aromatic residue in the GABA-binding pocket via a cation-π bond. Padgett *et al.* (2007) tested for this using unnatural amino acid substitution and found that a

tyrosine in the binding pocket, β_2Y97, participates in a cation-π bond that is immediately involved in GABA affinity. As a result they, very reasonably, concluded that β_2Y97 directly interacts with the amino group of GABA. However, the possibility remains that β_2Y97's cation partner is, instead, one of the multiple arginine residues located in the GABA binding pocket. These include α_1R67, α_1R120, α_1R132, and β_2R207, all of which have been shown to mediate GABA affinity (Westh-Hansen *et al.* 1999; Holden and Czajkowski 2002; Wagner *et al.* 2004; Laha and Wagner 2011).

Here, we utilized double-mutant cycle analysis to test for potential interactions between β_2Y97 and each of α_1R67, α_1R120, α_1R132, and β_2R207, by quantifying functional coupling in the context of changes in free energy that result from mutating amino acid residues in singles and in pairs. We also tested for functional coupling between each arginine and β_2F200, another aromatic residue located in the GABA-binding pocket that has been shown to influence GABA affinity (Wagner and Czajkowski 2001). Our results identify functional coupling between two of the arginines (α_1R132, β_2R207) and both β_2Y97 and β_2F200. Furthermore, we demonstrated an even tighter coupling between β_2Y97 and β_2F200. We concluded that β_2Y97 and β_2F200 form a single functional unit that is critical for GABA binding. The Y97/F200 pair could interact with the ammonium moiety of GABA via a cation-π bond and its position may be fine-tuned via secondary interactions with β_2R207 and/or α_1R132. Interestingly, by determining the binding rates of GABA, we provided direct evidence for the involvement of β_2Y97 and β_2F200 in GABA binding, for the first time. Last but not least, we found that neither α_1R67 nor α_1R120 is functionally coupled to the aromatics, ruling out any interactions thought to exist between them.

Materials and methods

cDNA constructs and mutagenesis

Human α_1, β_2, and γ_{2S} subunits were inserted into the pcDNA 3.1 vector. Desired subunit combinations were transiently expressed in HEK-293 cells by transfection of vectors containing the corresponding genes. An engineered β_2 variant ($\beta_{2\text{-GKER}}$) was originally used in order

Journal of Neurochemistry, Vol. 119, No. 2 (October 2011): pg. 283-293. DOI.

to rescue expression with $\alpha_1\beta_{2\text{-GKER}}$ receptors containing point mutations either on α_1 or β_2. $\beta_{2\text{-GKER}}$ has four amino acids of β_2 replaced with the aligned residues found on the β_3 subunit, D171G, N173K, T179E, and K180R (Taylor *et al.* 1999; Bollan *et al.* 2003). This subunit has been shown to assemble more efficiently (Bollan *et al.* 2003) and we have found no differences in kinetics, apparent GABA affinity ($EC_{50\text{-GABA}}$), or amplitude comparing to β_2-containing receptors. However, $\beta_{2\text{-GKER}}$ was later found insufficient to rescue expression for several mutations; in such instances, co-expression with the γ_{2S} subunit allowed rescue. For consistency, $\alpha_1\beta_{2\text{-GKER}}\gamma_{2S}$ receptors were used as the control in the present study. Mutant α_1 and β_2 subunits were created using the QuikChange II site-directed mutagenesis kit (Stratagene, La Jolla, CA), and double stranded sequencing of the entire coding region was conducted in order to verify fidelity.

Cell culture, transfection, and labeling

Human embryonic kidney (HEK-293) cells were cultured in Minimum Essential Medium Eagle with Earle's salts (Mediatech, Manassas, VA), supplemented with 10% newborn calf serum (Thermo Scientific, Waltham, MA) and Penicillin-Streptomycin-Glutamine (Mediatech) in a 37° C incubator under a 5% CO_2 atmosphere. Cells were plated onto 35 mm dishes coated with poly-L-lysine and were transfected 24 hours later using Lipofectamine 2000 (Invitrogen, Carlsbad, CA) with the following amounts of cDNAs: 500 ng of eGFP, 1 μg of α_1 (wild-type or mutant), 1 μg of $\beta_{2\text{-GKER}}$ (wild-type or mutant), and 3 μg of γ_{2S}. eGFP was used as a marker to identify transfected cells. Patch clamp recordings were carried out 48–72 hours post-transfection.

Electrophysiology

All recordings for this study were collected from outside-out patches excised from HEK-293 cells. GABA-evoked chloride currents were recorded from patches voltage clamped at −60 mV, at room temperature. Recordings were made using borosilicate glass pipettes filled with (in mM): 140 KCl, 10 EGTA, 2 MgATP, 20 phosphocreatine and 10 HEPES, pH 7.4. Rapid solution exchange was accomplished by using a multibarreled flowpipe array (Vitrodynamics, Rockaway, NJ)

mounted on a piezoelectric bimorph (Vernitron, Bedford, OH). A computer-controlled constant current source drove the bimorph to move solution interfaces over the patch with 10–90% exchange times of ~200 μs, as measured by the liquid junction current at the open pipette tip after each experiment. $GABA_A$ receptor agonists and antagonists were dissolved in the perfusion solution, which contains (in mM): 145 NaCl, 2.5 KCl, 2 CaCl2, 1 MgCl2, 10 HEPES, 4 mM Glucose, and pH 7.4. For extracellular solutions that contained more than 30 mM GABA, the concentration of NaCl was reduced to 95 mM, and a combination of sucrose and GABA was added to compensate for the reduced osmolarity. The pipette solution was adjusted in conjunction, reducing the KCl concentration to 90 mM, and 50 mM K-gluconate was added to maintain a constant Cl^- driving force. GABA and SR-95531 were obtained from Sigma-Aldrich Chemicals, St Louis, MO. Currents were low-pass filtered at 2–5 kHz with a four-pole Bessel filter and digitized at a rate no less than twice the filter frequency. Data were collected at 20 kHz using an Axopatch 200B amplifier (Axon Instruments, Foster City, CA) and an ITC-1600 digitizer (InstruTech, Port Washington, NY), controlled by Axograph X software (Axograph Scientific, Sydney, AUS). Macroscopic current ensembles were collected with 15-second intervals between consecutive solution applications.

Antagonist unbinding experiments

Outside-out patches were pre-equilibrated in SR-95531 for 750 ms, and then rapidly switched to a solution containing saturating GABA. The evoked current was shaped by the convolution of the time course of antagonist unbinding and the waveform of the control current (evoked with no pre-equilibration in antagonist). Home-written Matlab (Mathworks, Natick, MA) routines were used for the deconvolution of the time course of antagonist unbinding from this evoked current (Jones *et al.* 2001). The time course of antagonist unbinding was fit with an exponential function, yielding $k_{off\text{-}SR}$ and the percentage of receptors occupied by antagonist at equilibrium. The experiment was repeated several times, pre-equilibrating in different test concentrations of SR-95531. $K_{D\text{-}SR}$ was determined by plotting the antagonist occupancy versus concentration. The binding rate of SR-

Journal of Neurochemistry, Vol. 119, No. 2 (October 2011): pg. 283-293. DOI.

95531 ($k_{on\text{-}SR}$) was calculated from the known values of $k_{off\text{-}SR}$ and $K_{D\text{-}SR}$.

Measuring the microscopic binding rate of GABA

The microscopic binding rate of GABA ($k_{on\text{-}GABA}$) was measured using "race" experiments (Jones et al. 1998). In a race experiment, agonist (having an *unknown* binding rate) is co-applied with an antagonist, which has a previously determined binding rate ($k_{on\text{-}ant,}$ see *"Antagonist Unbinding Experiments" above*). The amplitude of the current evoked by co-application of agonist and antagonist is compared to the amplitude of current evoked by agonist alone, and this ratio ($I_{ag\text{-}ant}/I_{ag\text{-}only}$) is called I_{race}. I_{race} depends only on the relative concentrations and binding rates of agonist and antagonist. The only unknown is the agonist binding rate, $k_{on\text{-}agonist}$, which can be solved for using the following equation:

$$k_{\text{on agonist}} = [(\text{antagonist}) \cdot k_{\text{on ant}}]/[(\text{agonist}) \cdot (1/I_{\text{race}} - 1)]$$

Double-mutant cycle analysis

Mutant cycle analysis was performed on EC_{50} values and binding rates. $\Delta\Delta G'^{o}$ was calculated as RT ln ($k_{mutant}/k_{wild\text{-}type}$), where R is the ideal gas constant (1.987 calories/mole), T is the absolute temperature (296 K), and k is either $EC_{50\text{-}GABA}$ or $k_{on\text{-}GABA}$. EC_{50} values have been previously utilized to support side chain interactions and establish coupling coefficients (Kash *et al.* 2003; Price *et al.* 2007; Venkatachalan and Czajkowski 2008). If two mutations have independent effects, $\Delta\Delta G'^{o}_{(1,2)} = \Delta\Delta G'^{o}_{(1)} + \Delta\Delta G'^{o}_{(2)}$. For our evaluation, the further a coupling energy [$\Delta\Delta G'^{o}_{coupling} = \Delta\Delta G'^{o}_{(1,2)} - (\Delta\Delta G'^{o}_{(1)} + \Delta\Delta G'^{o}_{(2)})$] deviates from 0 kcal/mol the less functionally independent the two residues are from one another.

Statistical methods

Graphpad Prism 4 (GraphPad Software, Inc., San Diego, CA) was employed for fitting concentration-response curves and performing statistical significance test. For concentration-response

curves, relative mean ± SEM was plotted against the GABA concentration. The resulting plot was fitted with a form of the Hill equation, Y = Min + (Max − Min)/(1 + 10^((LogEC50 − X) * HillSlope)), where X is the log value of the GABA concentration. Significant differences between control and mutant parameters, where appropriate, were tested using ANOVA with a Dunnett's post-test, at a significant level of $p < 0.05$.

Results

The present study sought to employ double-mutant cycle analysis to test for potential interactions between arginines (α_1R67, α_1R120, α_1R132, and β_2R207) and aromatics (β_2Y97 and β_2F200) located in the $GABA_A$ receptor ligand-binding pocket. The targeted amino acid residues were mutated singly and in pairs. In order to achieve consistent expression, all of the mutations were expressed in a background of $\alpha_1\beta_{2\text{-GKER}}\gamma_{2s}$, which also served as our control construct (Bollan *et al.* 2003; Laha and Wagner 2011). For readability, the mutant constructs will be referred to as R67A, R120A, R132A, R207A, Y97A, F200I, R120A-Y97A, R120A-F200I, R132A-Y97A, R132A-F200I, R207A-Y97A, R207A-F200I, Y97A-F200I, and Y97A-F200I-R207A to indicate the corresponding single, double, or triple mutant receptor.

Each mutation tested increases $EC_{50\text{-GABA}}$

Each of the arginines and aromatics of interest was mutated to alanine and transiently expressed in HEK-293 cells, in order to record GABA-evoked currents from outside-out patches. $EC_{50\text{-GABA}}$ was determined by fitting concentration-response plots with a form of the Hill equation. Overall, $EC_{50\text{-GABA}}$ measured at peak response for every single and double mutant tested displayed a significant rightward shift ranging from 288 μM (4-fold, R132A) to 22.65 mM (310-fold, R207A-F200I) compared to control ($EC_{50\text{-GABA}}$ $\alpha_1\beta_{2\text{-GKER}}\gamma_{2S}$ = 73 μM) (Figure 1). These shifts in $EC_{50\text{-GABA}}$ values are entirely consistent with previously published results, which suggest each of these residues mediate GABA affinity.

Journal of Neurochemistry, Vol. 119, No. 2 (October 2011): pg. 283-293. DOI.

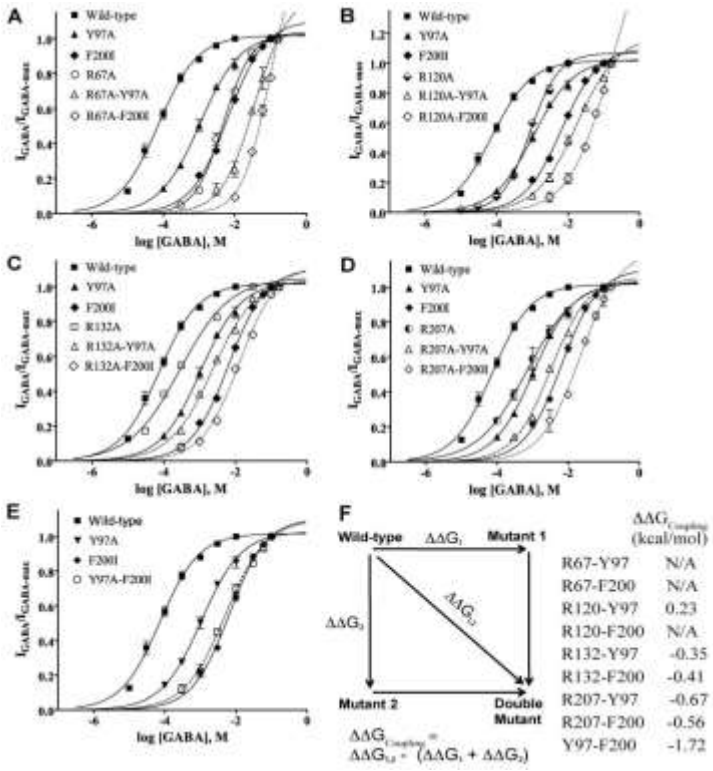

Figure 1 $EC_{50\text{-}GABA}$ double-mutant cycle analysis identified pairs of amino acid residues that are functionally coupled. $EC_{50\text{-}GABA}$ was obtained through concentration-response experiments in which the peak currents from a series of sub-saturating concentrations of GABA were compared to the peak currents at saturating GABA. The concentration-response plot was fit with a form of the Hill equation to obtain an EC_{50} value. A–D) Concentration response curves for wild-type, Y97A, and F200I; unique to each plot are the curves for specific arginine single mutant and the corresponding two double mutants containing that particular arginine. E) The double mutant Y97A-F200I concentration-response plot is identical to that of the single mutant F200I; both are right-shifted compared to wild-type. The concentration-response analysis yielded the following $EC_{50\text{-}GABA}$ values (in mM): wild-type, 0.073; R67A, 4.80; R120A, 0.85; R132A, 0.29; R207A, 0.70; Y97A, 1.06; F200I, 6.50; R120A-Y97A, 17.89; R132A-Y97A, 2.31; R132A-F200I, 12.93; R207A-Y97A, 3.26; R207A-F200I, 22.65; Y97A-F200I, 5.04. The $EC_{50\text{-}GABA}$ values could not be accurately determined for R67A-Y97A, R67A-F200I, and R120A-F200I double mutations. F) Double-mutant cycle analysis schematic and a summary of the coupling energies determined.

Because these $EC_{50\text{-}GABA}$ values are used to drive double-mutant cycle analysis in this study, it is crucial that accurate values of this parameter are determined for each construct analyzed. This can be particularly challenging for double-mutant constructs having $EC_{50\text{-}GABA}$ values >10 mM, which require GABA concentrations of 100 mM or greater to achieve saturation for the GABA-evoked current response.

Journal of Neurochemistry, Vol. 119, No. 2 (October 2011): pg. 283-293. DOI.

We found that we could get consistent results using GABA concentrations of up to 160 mM, but issues of osmotic imbalance across the patch precluded us from employing higher concentrations. Because of this, we could not accurately quantify $EC_{50\text{-}GABA}$ for some of the more severely shifted constructs (R67A/F200I, R67A/Y97A, and R120A/F200I). We confirmed that the GABA-evoked response was effectively saturated for each of the remaining constructs by analyzing the rise time of the initial activation phase of the current. The activation rate has a higher saturation point than the peak current amplitude (Li and Pearce 2000), and we verified that the activation rate for each mutant receptor reached a plateau (Figure 2).

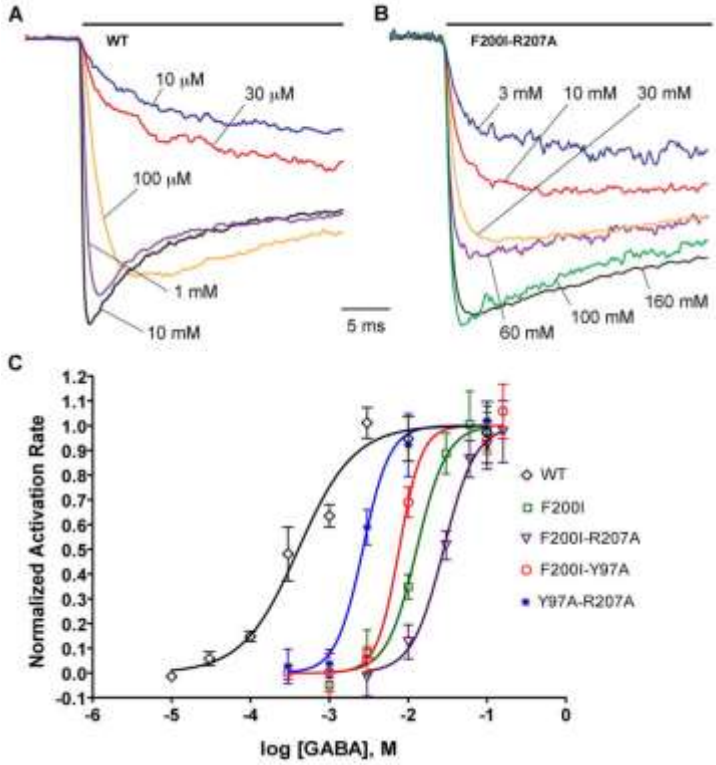

Figure 2 Activation phase of GABA-evoked current saturates at high GABA concentration. A) Overlayed raw wild-type currents activated by varying concentrations of GABA, from multiple patches. B) Overlayed raw F200I-R207A currents activated by varying concentrations of GABA, from multiple patches. In both, black horizontal bar indicates GABA application. The activation (rising) phase of each current was fit by a single-exponent equation, yielding an activation time constant ($\tau_{activation}$). $1/\tau_{activation}$ was used to calculate the activation rate. C) Plot of normalized activation rate of each receptor construct with respect to GABA concentration. Each plot was fit with a form of the Hill equation.

Journal of Neurochemistry, Vol. 119, No. 2 (October 2011): pg. 283-293. DOI.

In later experiments that depend on the competitive antagonist SR-95531, it was found that the β_2F200A mutation could not be used because it causes a debilitating reduction in SR-95531 affinity. Therefore, a milder mutation, β_2F200I, was tested. β_2F200I was found to adequately support SR-95531 binding and had less severe effects on $EC_{50\text{-}GABA}$ than β_2F200A, making it very useful for the double-mutant cycle analysis studies that followed.

Double-mutant cycle analysis of $EC_{50\text{-}GABA}$ reveals little coupling between the arginines from the α_1 subunit and β_2Y97 or β_2F200

This study aimed to assess the relationships between residues using the method of double-mutant cycle analysis. Double-mutant cycle analysis quantifies the extent of functional coupling between two residues by comparing the changes in free energy ($\Delta\Delta G$) resulting from single mutations and the corresponding double mutation, to measure the likelihood of two residues interacting (Horovitz 1996). One parameter that has been commonly used for double-mutant cycle analysis, in the study of proteins such as LGICs, is the apparent affinity for ligand, or the EC_{50} value (Kash *et al.* 2003; Price *et al.* 2007; Venkatachalan and Czajkowski 2008).

As a single mutation, R67A caused the largest shift in $EC_{50\text{-}GABA}$, and when combined with either Y97A or F200I even more severe shifts were observed (Figure 1A). Curve fits to the concentration-response data for either double mutant were not possible because the responses never approached saturation. In addition, for either double mutant, propofol-evoked currents (1 mM) displayed peak amplitudes greater than twice those evoked by 160 mM GABA (the highest concentration tested, data not shown), suggesting that $EC_{50\text{-}GABA}$ for either of these constructs is greater than 160 mM. Because we were not able to accurately quantify $EC_{50\text{-}GABA}$ for these constructs we could not subject them to double-mutant cycle analysis. However, the fact that the double mutations are so debilitating is suggestive that no functional coupling exists between α_1R67 and either β_2Y97 or β_2F200, and it is unlikely that α_1R67 shares an interaction with either aromatic residue.

Journal of Neurochemistry, Vol. 119, No. 2 (October 2011): pg. 283-293. DOI.

As was seen for R67A, when R120A was co-expressed with F200I, the effect on $EC_{50\text{-}GABA}$ was too severe to be quantified and the two residues are not likely to be functionally coupled. On the other hand, R120A-Y97A receptors displayed a measurable $EC_{50\text{-}GABA}$ (17.9 mM). This value, along with the $EC_{50\text{-}GABA}$ values for R120A (850 μM) and Y97A (1.06 mM), were used to drive double-mutant cycle analysis, which resulted in a coupling energy of 0.23 kcal/mol (Figure 1B, F). It should be noted that, double-mutant cycle analysis works on the premise that if two residues are perfectly independent, we would expect the coupling energy to be 0 kcal/mol. As such, any value that deviates from zero may indicate coupling. The further a coupling energy deviates from 0 kcal/mol the less functionally independent the two residues are from one another. Direct interactions typically have coupling energies that exceed |0.5 kcal/mol| (Kash *et al.* 2003; Price *et al.* 2007; Venkatachalan and Czajkowski 2008). Therefore, α_1R120 does not appear to be significantly coupled to β_2Y97 and it is not likely to participate in an interaction with either aromatic residue.

The double-mutant cycle analyses of R132A, with respect to Y97A and F200I, yielded modest coupling energies of −0.35 kcal/mol and −0.41 kcal/mol for R132-Y97 and R132-F200 pairs, respectively (Figure 1C, F). Although these coupling energies are not particularly strong, the values cannot be entirely disregarded and may indicate possible interactions. Interestingly, α_1R132 appears to be coupled to β_2Y97 and β_2F200 with the same magnitude.

Double-mutant cycle analysis of $EC_{50\text{-}GABA}$ reveals a ternary functional interaction between β_2R207, β_2Y97, and β_2F200

When R207A was co-expressed with Y97A or F200I, double mutant cycle analysis revealed significant coupling energies (−0.67 kcal/mol and −0.56 kcal/mol for the R207A-Y97A and R207A-F200I pairs respectively, Figure 1D, F). These coupling energies indicate that β_2R207 is tightly coupled to the aromatics, and it is possible that β_2R207 interacts with one or the other (i.e. via a cation-π bond).

We find it interesting that, as was also seen for α_1R132, β_2R207 is coupled to both β_2Y97 and β_2F200 to a similar degree. This similarity

in coupling would be predicted if β_2Y97 and β_2F200 are tightly linked structurally, effectively acting as a single functional unit. If this is the case, then double-mutant cycle analysis of the two aromatics should give a strong coupling energy. Indeed, the Y97A-F200I double mutation revealed a highly significant coupling energy (−1.72 kcal/mol) between β_2Y97 and β_2F200 (Figure 1E, F). Taken together, the strong coupling energies of β_2R207/β_2Y97, β_2R207/β_2F200, and β_2Y97/β_2F200 suggest that these three residues act together as single functional ternary complex to mediate GABA binding.

Triple mutant cycle analyses revealed unequal partnerships among ternary complex members: β_2R207, β_2Y97, and β_2F200

To further dissect the relationship between members of the ternary complex, we performed triple mutant cycle analyses. In other words, we carried out double mutant cycle analysis measuring coupling of two residues on the background of a third mutant. The only new data needed to perform this analysis was the $EC_{50\text{-}GABA}$ for the triple mutant, Y97A-F200I-R207A. This construct displayed robust GABA-evoked current and caused a 305-fold decrease in GABA affinity, ($EC_{50\text{-}GABA}$ = 22.2 mM). When double-mutant cycle analysis was applied to β_2Y97 and β_2F200 in a R207A background, strong coupling was still observed ($\Delta\Delta G_{Coupling}$ = −0.92 kcal/mol, Figure 3C). However, strong coupling of β_2R207 with β_2Y97 disappeared when tested on the F200I background ($\Delta\Delta G_{Coupling}$ = 0.14 kcal/mol, Figure 3A), as did coupling of β_2R207 with β_2F200 on the Y97A background ($\Delta\Delta G_{Coupling}$ = 0.21kcal/mol, Figure 3B). These coupling energies indicate that the presence of both β_2Y97 and β_2F200 is necessary for β_2R207's participation in the ternary complex. On the other hand, the presence of β_2R207 is not absolutely necessary for the functional interaction between β_2Y97 and β_2F200, despite a slight reduction in coupling energy.

Journal of Neurochemistry, Vol. 119, No. 2 (October 2011): pg. 283-293. DOI.

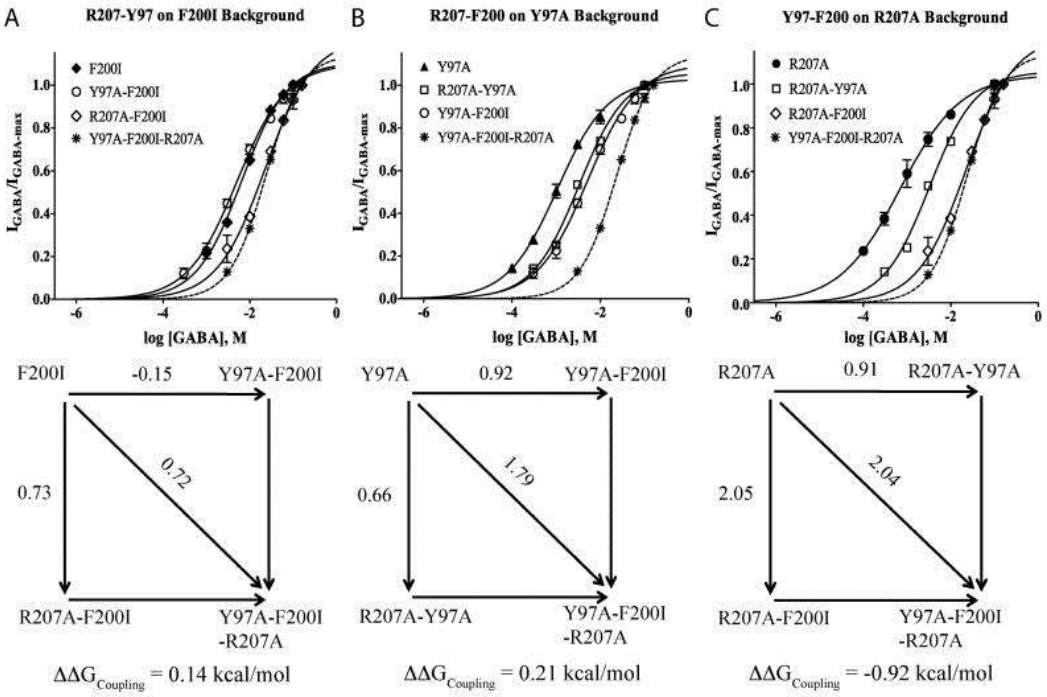

Figure 3 Functional coupling between β_2R207 and one of the two aromatic residues exists only in the presence of the other aromatic residue. Top row shows concentration response curves comparing the effects on GABA affinity caused by double mutants and triple mutant in the background of a single mutant control. Bottom row shows the double-mutant cycle analyses and the resulting coupling energies. A) β_2R207 is not functionally coupled to β_2Y97 when β_2F200 is mutated. B) β_2R207 is not functionally coupled to β_2F200 when β_2Y97 is mutated. C) β_2Y97 and β_2F200 remains coupled when β_2R207 is mutated.

Coupling between β_2R207, β_2F200, and β_2Y97 mediates GABA binding

While $EC_{50\text{-}GABA}$ is a useful parameter for driving double-mutant cycle analysis, it represents a complex interaction between several microscopic processes (i.e. ligand binding/unbinding, channel opening/closing, desensitization/resensitization) (Colquhoun 1998; Gleitsman *et al.* 2008). Therefore, we thought it would be informative to directly measure the GABA binding rate ($k_{on\text{-}GABA}$) for each construct and repeat double-mutant cycle analysis using this microscopic parameter. Such direct evidence for a residue's participation in GABA binding was previously demonstrated for β_2R207 (Wagner *et al.* 2004) but has not been done for β_2Y97 and β_2F200.

Journal of Neurochemistry, Vol. 119, No. 2 (October 2011): pg. 283-293. DOI.

$k_{on\text{-}GABA}$ was measured as previously described by Jones *et al.* (2001). Briefly, this process first involves determining the binding rate for a competitive antagonist, in this case SR-95531 (Supplemental Figure 1). Once the binding rate for SR-95531 ($k_{on\text{-}SR}$) is obtained, the binding rate of GABA can be determined by performing an experiment in which GABA and SR-95531 are co-applied, known as a race experiment. The resulting co-application current is compared to the current evoked by the application of GABA alone. The extent to which the peak current is reduced by the presence of the antagonist depends on the relative binding rates of the two compounds and the relative concentrations available. $k_{on\text{-}SR}$ is determined by the antagonist unbinding experiment, and then $k_{on\text{-}GABA}$ is calculated as $k_{on\text{-}GABA}$ = [SR-95531] $k_{on\text{-}SR}$/([GABA](1/I_{race} −1)) (Jones *et al.* 1998). I_{race} is the ratio of the peak response of co-application to the peak response of GABA alone.

The effects of each single mutant and double mutant receptor on the kinetics of SR-95531 and $k_{on\text{-}GABA}$ are summarized in Table 1. Alanine substitution at β_2R207 had no effect on $K_{D\text{-}SR}$. On the other hand, mutation of β_2F200 and β_2Y97 strongly affected SR-95531 affinity causing 55 and 20-fold increases in $K_{D\text{-}SR}$, respectively. This result supports the idea that β_2Y97 and β_2F200 are a tightly coupled functional group. Also, both β_2Y97 and β_2F200, as well as β_2R207, influence the $k_{on\text{-}GABA}$. Results from application of the $k_{on\text{-}GABA}$ values to double-mutant cycle analysis generally agreed with those seen from $EC_{50\text{-}GABA}$ (Figure 4). β_2Y97 and β_2F200 remain coupled ($\Delta\Delta G_{Coupling}$ = 1.09 kcal/mol), as do β_2R207 and β_2F200 ($\Delta\Delta G_{Coupling}$ = 0.56 kcal/mol). The coupling energy for β_2R207 and β_2Y97 dropped slightly to 0.40 kcal/mol, but is high enough that a potential interaction that mediates GABA binding remains possible. These results show that β_2Y97, β_2F200, and β_2R207 likely form a ternary complex that mediates GABA binding.

Journal of Neurochemistry, Vol. 119, No. 2 (October 2011): pg. 283-293. DOI.

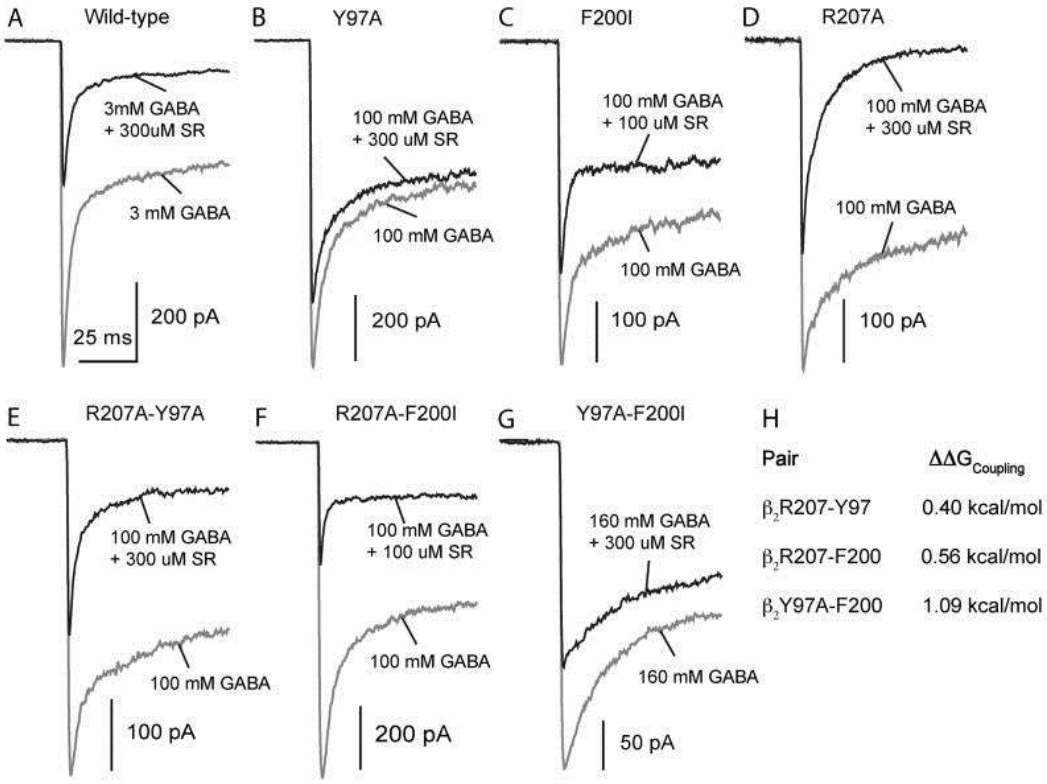

Figure 4 Functional coupling between β_2Y97, β_2F200, and β_2R207 at the microkinetic level ($k_{on\text{-}GABA}$). A–G) Sample raw traces recorded from race experiments. The solution exchange protocol was designed to alternate between control (only GABA, 500ms, gray) and test (GABA and SR-95531 simultaneously, 500ms, black) every 15 seconds. The known concentrations of GABA and SR and the ratio of GABA+SR: GABA only (I_{Race}) were used to calculate $k_{on\text{-}GABA}$ (see methods). H) Summary of the coupling energies determined from applying the $k_{on\text{-}GABA}$ values to double-mutant cycle analysis.

Table 1 Summary of results from antagonist unbinding and race experiments

	$K_{D\text{-}SR}$ (μM)	$k_{off\text{-}SR}$ (s^{-1})	$k_{on\text{-}SR}$ ($M^{-1}s^{-1}$)	$k_{on\text{-}GABA}$ ($M^{-1}s^{-1}$)	$\Delta\Delta G_{Coupling}$ (kcal/mol)
Wild-type	0.14	15.9 ± 0.8	$1.14 \pm 0.10 \times 10^8$	$7.40 \pm 0.40 \times 10^8$	–
Y97A	7.68	832.1 ± 91.5	$1.08 \pm 0.12 \times 10^8$	$2.17 \pm 0.11 \times 10^8$	–
F200I	2.79	331.0 ± 34.6	$1.19 \pm 0.12 \times 10^8$	$2.85 \pm 0.14 \times 10^8$	–
R207A	0.13	22.7 ± 3.6	$1.71 \pm 0.27 \times 10^8$	$9.16 \pm 0.35 \times 10^8$	–
Y97A-F200I	8.79	1159.5 ± 159	$1.32 \pm 0.18 \times 10^8$	$5.39 \pm 0.41 \times 10^8$	1.09
R207A-Y97A	0.97	151.7 ± 44.9	$1.57 \pm 0.46 \times 10^8$	$5.30 \pm 0.63 \times 10^8$	0.40
R207A-F200I	2.87	394.2 ± 56.2	$1.37 \pm 0.20 \times 10^8$	$9.28 \pm 0.46 \times 10^4$	0.56

Discussion

Cation-π bonding has been demonstrated to be a universal structural motif in proteins. In a cation-π bond the π orbital electrons

Journal of Neurochemistry, Vol. 119, No. 2 (October 2011): pg. 283-293. DOI.

from aromatic amino acid side chain (Trp, Tyr, Phe) interact with a cation. The cation may be provided by a basic residue (Arg, Lys, His) on the same subunit as the aromatic residue (Gallivan and Dougherty 1999), a basic residue from a different subunit (Crowley and Golovin 2005), or a positively charged exogenous ligand (Zacharias and Dougherty 2002). Cation-π bonds have been demonstrated to be key players in ligand binding for all members of the cys-loop LGIC family (Zhong *et al.* 1998; Beene *et al.* 2002; Lummis *et al.* 2005; Padgett *et al.* 2007; Pless *et al.* 2008).

At least five aromatic residues from the $GABA_A$ receptor (α_1F65, β_2Y97, β_2Y157, β_2F200, and β_2Y205) have been implicated in ligand binding (Sigel *et al.* 1992; Boileau *et al.* 1999; Boileau *et al.* 2002; Amin and Weiss 1993; Wagner and Czajkowski 2001). Padgett *et al.* (2007) demonstrated that one of these, β_2Y97, participates in a cation-π bond that mediates ligand binding and that α_1F65, β_2Y157, and β_2Y205 do not participate in functionally important cation-π interactions. The remaining aromatic, β_2F200, remains untested for cation-π interaction.

In this study we employed double-mutant cycle analysis to test for possible interactions among candidate residues that have cation-π ability at the GABA-binding pocket. Functional coupling between either β_2Y97 or β_2F200 and each of the arginines present in the GABA-binding pocket (α_1R67, α_1R120, α_1R132, and β_2R207) was measured. Our results identify α_1R132 and $\beta_2$207 as potential cation-π partners for each of the aromatics, and rule out α_1R67 and α_1R120. In addition, a strong and consistent coupling was identified between the two aromatics themselves, suggesting that β_2Y97 and β_2F200 directly interact.

β_2Y97 and β_2F200 as a tight aromatic pair

The clearest result from this study is that β_2Y97 and β_2F200 work together as a single functional unit. When double-mutant cycle analysis, using $EC_{50\text{-}GABA}$, was employed to test for coupling between β_2R207 and either β_2Y97 or β_2F200, the results were comparable ($\Delta\Delta G_{Coupling}$: R207/Y97 = −0.67 kcal/mol, R207/F200 = −0.56

kcal/mol). Similarly, α_1R132 was found to be equally coupled to each aromatic residue ($\Delta\Delta G_{Coupling}$: R132/Y97 = −0.35 kcal/mol, R132/F200 = −0.41 kcal/mol). These results strongly suggest that β_2Y97 and β_2F200 work in concert. This hypothesis is supported by the fact that the two residues are strongly coupled to each other when the mutational effects on $EC_{50\text{-}GABA}$ ($\Delta\Delta G_{Coupling}$ Y97/F200 = −1.72 kcal/mol), $k_{on\text{-}GABA}$ ($\Delta\Delta G_{Coupling}$ Y97/F200 = 1.09 kcal/mol) and $k_{off\text{-}SR}$ ($\Delta\Delta G_{Coupling}$ = −1.59 kcal/mol) are used to drive the double-mutant cycle analysis. Furthermore, mutation of either residue had qualitatively similar effects on every parameter we measured: $EC_{50\text{-}GABA}$, $k_{off\text{-}SR}$, $k_{on\text{-}SR}$, and $k_{on\text{-}GABA}$.

Another line of evidence supporting a tight interaction between β_2Y97 and β_2F200 comes from the fact that coupling between β_2R207 and each aromatic was abolished when tested in a background where the other aromatic residue had been mutated. In other words, whatever interaction β_2R207 might share with β_2Y97 disappears when β_2F200 is mutated, and whatever interaction β_2R207 shares with β_2F200 disappears when β_2Y97 is mutated. Conversely, the coupling energy between β_2Y97 and β_2F200 is only modestly reduced by mutation of β_2R207.

Taken altogether, these results suggest that β_2Y97 and β_2F200 form a single functional unit that then interacts with β_2R207 and possibly α_1R132. It is likely that these interactions between β_2R207, α_1R132, and the Y97/F200 complex occur via a cation-π bond(s) with either aromatic, but it is also possible that the interaction of β_2Y97 and β_2F200 positions other elements (i.e. neighboring side chains or backbone carbonyls) for interactions with either of the arginines.

The role of arginines from the α_1 subunit

Of the arginines from the α_1 subunit that were tested, we found that α_1R132 can potentially interact with either β_2Y97 or β_2F200 but that neither α_1R67 nor α_1R120 is likely to participate in any interactions with either of the two aromatics. When expressed as a single mutation, α_1R132A has relatively moderate effects on $EC_{50\text{-}GABA}$ (4-fold increase), suggesting that it might act to help position the more critical Y97/F200 pair rather than directly coordinating the GABA

Journal of Neurochemistry, Vol. 119, No. 2 (October 2011): pg. 283-293. DOI.

molecule. The lack of an interaction between α_1R120 and the aromatics is not particularly surprising. According to the homology model, α_1R120 is relatively distant from the aromatics and it has been proposed to participate in a state-dependent inter-subunit salt bridge with β_2D163 (Cromer *et al.* 2002; Laha and Wagner 2011). The fact that α_1R67 does not interact with the aromatics examined here but is located nearby and, on its own, severely affects GABA affinity suggest that it plays a critical role in GABA binding that is independent of the Y97/F200 pair.

A model of the GABA binding pocket

The current best structural model of the $GABA_A$ receptor ligand-binding pocket is the homology model that has been developed based on the crystal structure of the molluscan acetylcholine binding protein (AChBP) (Brejc *et al.* 2001; Cromer *et al.* 2002; O'Mara *et al.* 2005). In this homology model the distance between the aromatic rings of β_2Y97 and β_2F200 ranges from 6–9 angstroms when the side chains are rotated through their stable conformations. This distance is too great to support direct aromatic-aromatic interaction and may appear to be evidence against the tight Y97/F200 interaction proposed here. However, β_2F200 is located at the apex of Loop C, a region that aligns very poorly with the AChBP (Cromer *et al.* 2002) and whose actual structure is likely to differ significantly from the AChBP structure (Ernst *et al.* 2003). In addition, Loop C appears to be quite flexible (Wagner and Czajkowski 2001; Bourne *et al.* 2010). Therefore, we believe the results presented here have provided a new constraint on the homology model and that future versions of the model should attempt to translate the alpha carbon of β_2F200 a few angstroms so that it can interact with β_2Y97. Figure 5 illustrates a possible orientation of GABA at the binding pocket.

Journal of Neurochemistry, Vol. 119, No. 2 (October 2011): pg. 283-293. DOI.

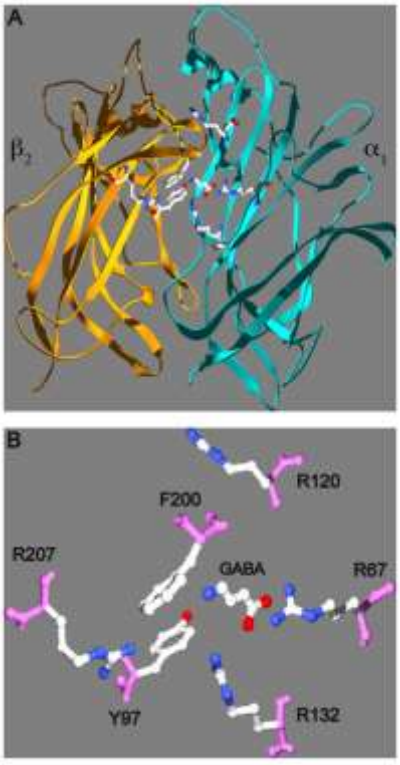

Figure 5 Interpretation of our results at the GABA binding pocket: a model of the GABA binding pocket based on the homology structure proposed by Cromer *et al.* (2002). A) Side-view of β/α interface showing the side chains of all the residues mutated in this study. GABA has been manually placed in its proposed orientation between R67 and F200/Y97. B) Zoomed view of panel A with backbone removed. The alpha carbon of each residue has not been moved from its original position in the homology model (Cromer *et al.* 2002). Several of the side chains have been rotated to alternate stable positions (using the mutate function in Swiss PDB viewer). The side chain of F200 has been slightly rotated using the torsion function in Swiss PDB viewer.

The proposed stacking interaction between β_2Y97 and β_2F200 could leave the alternate faces available for cation-π bonding with the amino group of GABA. Because β_2F200 has significantly stronger effects on GABA affinity, we propose that it serves as a docking point for the GABA amino group. This leaves β_2Y97 available for cation-π interaction with β_2R207 or α_1R132. The homology model ideally positions α_1R132 for this interaction. Therefore, in our model we choose to depict it thusly, and show β_2R207 contributing via interaction(s) with the backbone carbonyl of β_2Y97, which it perfectly reaches according to the homology model.

Journal of Neurochemistry, Vol. 119, No. 2 (October 2011): pg. 283-293. DOI.

So far, this model leaves the question of where the carboxyl group of GABA docks. The guanidinium group of an arginine could serve as the docking site for the GABA carboxyl group. Specifically, α_1R67 has previously been proposed as a potential docking site for this moiety (Padgett *et al.* 2007). This hypothesis is supported by the fact that, of the four arginines tested here, mutation of α_1R67 to alanine has the largest effects on both the GABA binding rate and the GABA unbinding rate (unpublished data). Furthermore, α_1R67A and β_2F200I, as single mutations, have the most severe effects on GABA affinity and these effects appear fully additive in the R67A-F200I double mutant. This result supports a model in which α_1R67 and β_2F200 serve as critical and independent sites that coordinate the carboxyl end and the amino end of GABA respectively.

Acknowledgments

This research was supported by the National Institutes of Health [Grant NS055793].

Abbreviations

$GABA_A$	γ-aminobutyric acid type A
LGIC	ligand-gated ion channel

Footnotes

There is no conflict of interest.

About the Authors:

Corresponding Author: Phu N. Tran, Marquette University, Department of Biological Sciences, P.O. Box 1881, Milwaukee, Wisconsin 53201-1881, USA, Phone: (414) 288–5695, Fax: (414) 288–7357, Email: phu.tran@marquette.edu, or ; Email: pntran@wisc.edu

Authorship Contributions

Participated in research design: Tran, Laha, and Wagner.

Conducted experiments: Tran and Laha.

Performed data analysis: Tran and Laha.

Wrote or contributed to the writing of the manuscript: Tran, Laha and Wagner.

Other: Wagner acquired funding for the research.

References

Amin J, Weiss D. GABAA receptor needs two homologous domains of the β subunit for activation by GABA, but not by pentobarbital. Nature. 1993;366:565–569.

Baumann SW, Baur R, Sigel E. Forced subunit assembly in alpha1 beta2gamma2 GABAA receptors. Insight into the absolute arrangement. J Biol Chem. 2002;277:46020–5.

Beene DL, Brandt GS, Zhong W, Zacharias NM, Lester HA, Dougherty DA. Cation-pi interactions in ligand recognition by serotonergic (5-HT3A) and nicotinic acetylcholine receptors: the anomalous binding properties of nicotine. Biochemistry. 2002;41:10262–9.

Benke D, Fritschy JM, Trzeciak A, Bannwarth W, Mohler H. Distribution, prevalence, and drug binding profile of gamma-aminobutyric acid type A receptor subtypes differing in the beta-subunit variant. J Biol Chem. 1994;269:27100–7.

Boileau AJ, Evers AR, Davis AF, Czajkowski C. Mapping the agonist binding site of the GABAA receptor: evidence for a β-strand. J Neurosci. 1999;19:4847–54.

Boileau AJ, Newell JG, Czajkowski C. GABAA receptor β2 Tyr97 and Leu99 line the GABA-binding site: insights into mechanisms of agonist and antagonist actions. J Biol Chem. 2002;277:2931–7.

Bollan K, King D, Robertson LA, Brown K, Taylor PM, Moss SJ, Connolly CN. GABA(A) receptor composition is determined by distinct assembly signals within alpha and beta subunits. J Biol Chem. 2003;278:4747–55.

Bourne Y, Radic Z, Araoz R, Talley TT, Benoit E, Servent D, Taylor P, Molgo J, Marchot P. Structural determinants in phycotoxins and AChBP conferring high affinity binding and nicotinic AChR antagonism. Proc Natl Acad Sci USA. 2010;107:6076–81.

Brejc K, van Dijk WJ, Klaassen RV, Schuurmans M, van Der Oost J, Smit AB, Sixma TK. Crystal structure of an ACh-binding protein reveals the ligand-binding domain of nicotinic receptors. Nature. 2001;411:269–76.

Colquhoun D. Binding, gating, affinity and efficacy: the interpretation of structure-activity relationships for agonists and of the effects of mutating receptors. Br J Pharmacol. 1998;125:924–47.

Cromer BA, Morton CJ, Parker MW. Anxiety over GABA(A) receptor structure relieved by AChBP. Trends Biochem Sci. 2002;27:280–7.

Crowley PB, Golovin A. Cation-π interactions in protein–protein interfaces. Proteins. 2005;59:231–9.

Ernst M, Brauchart D, Boresch S, Sieghart W. Comparative modeling of GABA(A) receptors: limits, insights, future developments. Neuroscience. 2003;119:933–43.

Gleitsman KR, Kedrowski SM, Lester HA, Dougherty DA. An intersubunit hydrogen bond in the nicotinic acetylcholine receptor that contributes to channel gating. J Biol Chem. 2008;283:35638–43.

Holden JH, Czajkowski C. Different residues in the $GABA_A$ receptor α_1T60–α_1K70 region mediate GABA and SR-95531 actions. J Biol Chem. 2002;277:18785–92.

Horovitz A. Double-mutant cycles: a powerful tool for analyzing protein structure and function. Fold Des. 1996;1:121–6.

Jones MV, Sahara Y, Dzubay JA, Westbrook GL. Defining affinity with the GABAA receptor. J Neurosci. 1998;18:8590–8604.

Jones MV, Jonas P, Sahara Y, Westbrook GL. Microscopic kinetics and energetics distinguish GABA(A) receptor agonists from antagonists. Biophys J. 2001;81:2660–70.

Kash TL, Jenkins A, Kelley JC, Trudell JR, Harrison NL. Coupling of agonist binding to channel gating in the GABA(A) receptor. Nature. 2003;421:272–5.

Kash TL, Trudell JR, Harrison NL. Structural elements involved in activation of the gamma-aminobutyric acid type A (GABAA) receptor. Biochem Soc Trans. 2004;32:540–6.

Laha KT, Wagner DA. A state-dependent salt-bridge interaction exists across the β/α intersubunit interface of the $GABA_A$ receptor. Mol Pharm. 2011 doi: 10.1124/mol.110.068619.

Li X, Pearce RA. Effects of halothane on $GABA_A$ receptor kinetics: evidence for slowed agonist unbinding. J Neurosci. 2000;20:899–907.

Lummis SC, Beene D, Harrison NJ, Lester HA, Dougherty DA. A cation-π interaction with a tyrosine in the binding site of the GABAC receptor. Chem Biol. 2005;12:993–7.

Lummis SCR. Locating GABA in GABA receptor binding sites. Biochem Soc Trans. 2009;37:1343–6.

McKernan RM, Whiting PJ. Which GABAA-receptor subtypes really occur in the brain? Trends Neurosci. 1996;19:139–43.

O'Mara M, Cromer B, Parker M, Chung SH. Homology model of the GABAA receptor examined using Brownian dynamics. Biophys J. 2005;88:3286–99.

Padgett CL, Hanek AP, Lester HA, Dougherty DA, Lummis SC. Unnatural amino acid mutagenesis of the GABA(A) receptor binding site residues reveals a novel cation-pi interaction between GABA and beta2Tyr97. J Neurosci. 2007;27:886–892.

Pless SA, Millen KS, Hanek AP, Lynch JW, Lester HA, Lummis SCR, Dougherty DA. A Cation-π interaction in the binding site of the glycine receptor is mediated by a phenylalanine residue. J Neurosci. 2008;28:10937–42.

Price KL, Millen KS, Lummis SC. Transducing agonist binding to channel gating involves different interactions in 5-HT3 and GABAC receptors. J Biol Chem. 2007;282:25623–30.

Sigel E, Baur R, Kellenberger S, Malherbe P. Point mutations affecting antagonist affinity and agonist dependent gating of $GABA_A$ receptor channels. EMBO J. 1992;11:2017–23.

Taylor PM, Thomas P, Gorrie GH, Connolly CN, Smart TG, Moss SJ. Identification of amino acid residues within GABA(A) receptor beta subunits that mediate both homomeric and heteromeric receptor expression. J Neurosci. 1999;19:6360–71.

Venkatachalan SP, Czajkowski C. A conserved salt bridge critical for GABA(A) receptor function and loop C dynamics. Proc Natl Acad Sci USA. 2008;105:13604–13609.

Wagner DA, Czajkowski C. Structure and dynamics of the GABA binding pocket: A narrowing cleft that constricts during activation. J Neurosci. 2001;21:67–74.

Wagner DA, Czajkowski C, Jones MV. An arginine involved in GABA binding and unbinding but not gating of the GABA(A) receptor. J Neurosci. 2004;24:2733–41.

Westh-Hansen SE, Witt MR, Dekermendjian K, Liljefors T, Rasmussen PB, Nielsen M. Arginine residue 120 of the human GABAA receptor alpha 1, subunit is essential for GABA binding and chloride ion current gating. Neuroreport. 1999;10:2417–21.

Zacharias N, Dougherty DA. Cation-π interactions in ligand recognition and catalysis. Trends in Pharmacological Sciences. 2002;23:281–7.

Zhong W, Gallivan JP, Zhang Y, Li L, Lester HA, Dougherty DA. From ab initio quantum mechanics to molecular neurobiology: a cation-pi binding site in the nicotinic receptor. Proc Natl Acad Sci USA. 1998;95:12088–93.

Supplementary Material

Supplemental Figure 1. Antagonist unbinding experiments. A) Sample raw traces recorded from antagonist unbinding experiments. Solution exchange protocol was designed to go in the sequence of 500 ms in saturating GABA solution, 15 seconds in wash, then 500 ms in a test concentration of SR-95531 followed immediately by 500 ms in saturating GABA solution, back to wash for 15 seconds, and the cycle repeats. The resulting raw data was analyzed to determine the microscopic kinetics, K_D, k_{off}, and k_{on}, for SR-95531. The sample raw traces show current resulted from control GABA (blue) and pre-equilibration (red). B) Deconvolution of GABA-evoked currents after SR-95531pre-equilibration from control currents (no pre-equilibration) reveals the time course of SR-95531 unbinding. Deconvolutions were fit to the equation

$$A(t) = [P_\infty - (P_\infty - P_0)\exp(-t/\tau_u)]^N,$$

where A(t) is the fraction of available receptors (antagonist not bound at any site), P_0 and P_∞ are the probabilities that a single binding site is available initially at t = 0 and at steady state as $t \rightarrow \infty$, τ_u is the time constant of antagonist unbinding from each site ($k_{off\text{-}SR} = 1/\tau_u$), and N is the number of binding sites (Jones *et al*. 2001). C) Concentration-response curves, for the equilibrium antagonist occupancy in the absence of GABA A(t = 0), were fit to the normalized hill equation $I/I_{max} = 1 - 1/[(K_{D\text{-}SR}/[\text{SR-95531}])^N + 1]$.

Journal of Neurochemistry, Vol. 119, No. 2 (October 2011): pg. 283-293. DOI.

Supplemental Figure 1

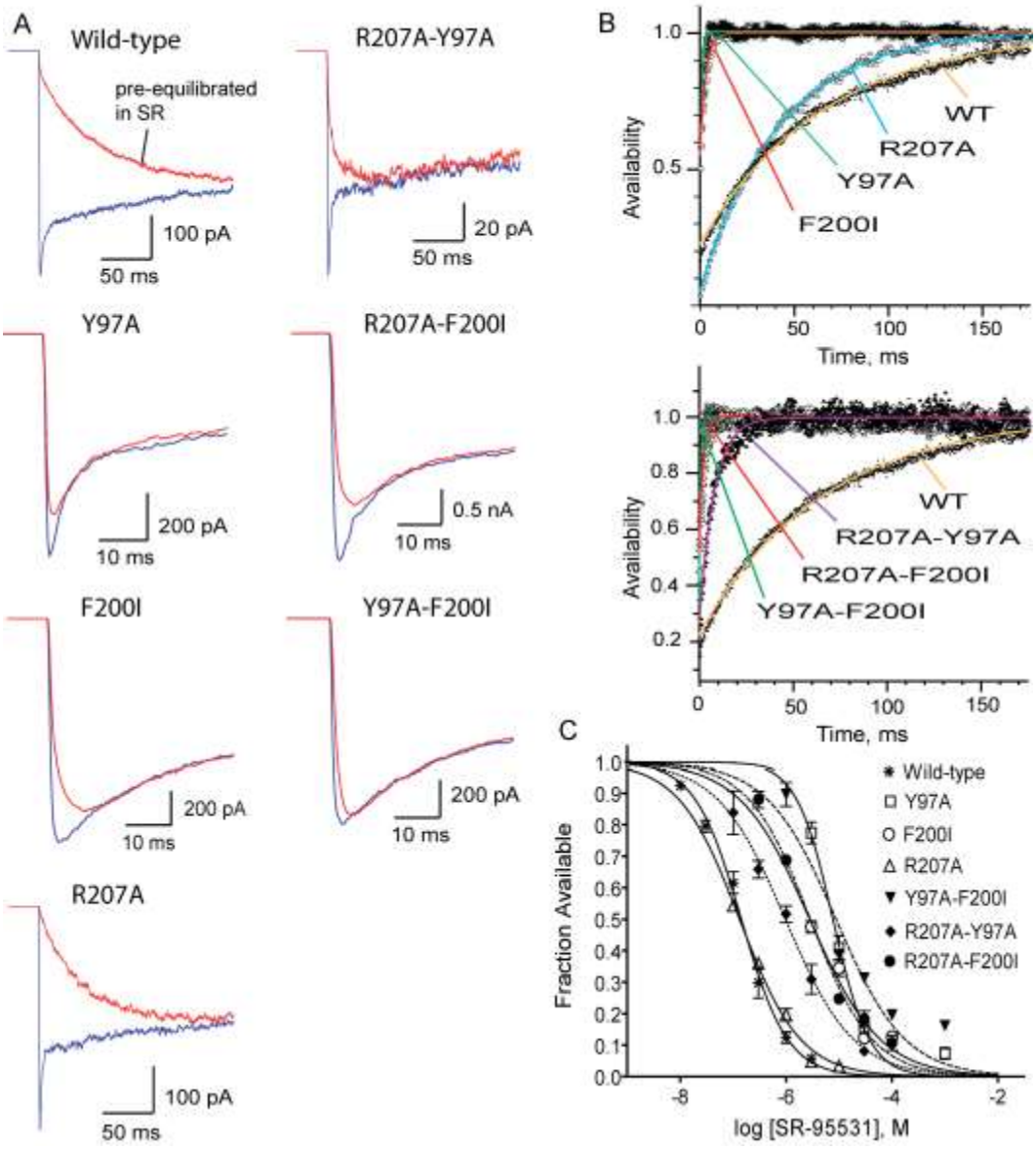

Journal of Neurochemistry, Vol. 119, No. 2 (October 2011): pg. 283-293. DOI.